Catalysis Communications 41 (2013) 41–46

Contents lists available at SciVerse ScienceDirect

Catalysis Communications

journal homepage: www.elsevier.com/locate/catcom

Short Communication

Hydrodeoxygenation of p-cresol on unsupported Ni–P catalysts prepared by thermal decomposition method

Weiyan Wang, Kun Zhang, Huan Liu, Zhiqiang Qiao, Yunquan Yang *, Kai Ren

School of Chemical Engineering, Xiangtan University, Xiangtan City, Hunan 411105, PR China

ARTICLE INFO

Article history:
Received 20 April 2013
Received in revised form 6 June 2013
Accepted 2 July 2013
Available online 9 July 2013

Keywords:
Hydrodeoxygenation
Ni_2P catalyst
Thermal decomposition
p-cresol
Bio-oil

ABSTRACT

Unsupported Ni–P catalysts were prepared from the mixed precursor of $NiCl_2$ and NaH_2PO_2 by thermal decomposition method, and their catalytic activities were measured using the hydrodeoxygenation (HDO) of p-cresol as probe. The effects of the $H_2PO_2^-/Ni^{2+}$ molar ratio in the precursor and the thermal decomposition temperature on the catalyst purity, crystallite size and HDO activity were studied. The HDO of p-cresol on these Ni–P catalysts proceeded with two parallel pathways yielding methylbenzene and methylcyclohexane as final products. The higher HDO catalytic activity of the catalyst was attributed to its bigger crystallite size and purer phase of Ni_2P.

1. Introduction

Owing to the decline in the availability of crude oil resources, bio-oil from the fast pyrolysis of lignocellulosic biomass was considered to be an alternative source for green and renewable fuel because it could reduce the world's dependency on fossil fuel and contribute no new carbon dioxide to the atmosphere [1,2]. However, this bio-oil contains very important amount of oxygenated compounds, which results in its immiscibility with crude oil and low heating value [3]. To expand the utilization of bio-oil as supplements or replacements for gasoline or fossil diesel, it is necessary to selectively remove oxygen [4]. Hydrodeoxygenation (HDO), a promising technology, has been intensively investigated for the upgrading bio-oil in recent years [5].

There have appeared many HDO catalysts in the literatures, including noble catalysts [6,7], sulfide catalysts [8,9], phosphide catalysts [10,11] and others [12,13]. Of these catalysts, sulfide catalysts are the traditional hydrotreating catalysts, which were widely applied in hydrodesulfurization (HDS) [14,15], hydrodenitrogenation (HDN) [16,17] and hydrodeoxygenation (HDO) [8,9,18]. But for HDO, because of a very low of sulfur in the bio-oil and a negative effect of oxygen for the sulfide structure, it needs to add some sulfiding agent into the feed to maintain the HDO activity of sulfide catalysts [19]. Noble metal catalysts exhibited higher HDO activity than sulfide catalysts, but the high cost prevents their wide practical application. However, metal phosphide catalysts had shown high activity for the HDS and HDN reactions as compared to the traditional Co(Ni)–Mo–S catalysts and possessed higher thermal stabilities as compared to nitride catalysts [20]. Yang et al. [21] had reported that CoMoP/MgO catalyst was a good candidate for the HDO of phenol, and the deoxygenation rate was increased drastically with the reaction temperature. Recently, Zhao et al. [11] had found that metal phosphide catalyst was superior active for the HDO reactions as compared to the traditional molybdenum sulfide catalysts and the commercial 5% Pd/Al_2O_3 catalyst. Moreover, they had also confirmed that the activity of metal phosphides followed the order Ni_2P > WP > MoP > CoP > FeP for the HDO of a biofuel model compound [22].

At present, the prepared method of Ni_2P catalyst for the HDO reaction was mainly concentrated on the TPR method [10,11]. This method requires a high temperature (600–650 °C) and a long treatment time due to the strong P–O bond in the phosphate, which leads to a serious agglomeration and relatively low activity. Ni_2P catalysts prepared by thermal decomposition had exhibited a high activity in the hydrodesulfurization (HDS) [23,24]. It had been also reported that there was a strong interaction with the Ni_2P particles and supports, and the supports' performance had great influence for the catalytic activity of the supported catalysts [25,26]. Therefore, to eliminate the effects of supports on the catalytic properties, we synthesized unsupported Ni_2P catalyst from the mixed precursors of nickel chloride and sodium hypophosphite by thermal decomposition and focused on the effects of the preparation

* Corresponding author. Tel.: +86 731 58298581; fax: +86 731 58293284.
E-mail address: yangyunquan@xtu.edu.cn (Y. Yang).

1566-7367
http://dx.doi.org/10.1016/j.catcom.2013.07.003

condition of the catalysts on their catalytic activities in the HDO of p-cresol.

2. Experimental

2.1. Catalyst preparation

All solvents and reagents were obtained from Sinopharm Chemical Reagent Co., Ltd. in high purity (≥99%) and used without further purification. Unsupported nickel phosphide catalysts were synthesized by directly thermal decomposition method. $NiCl_2$ (4 mmol) and a certain amount of NaH_2PO_2 were dissolved in water under ultrasonic environment. Subsequently, a solid precursor was obtained after the solution was evaporated slowly. Then, the precursor was directly heated to the required temperature for 1.0 h in a flowing 30 mL/min N_2. Finally, the product was cooled to ambient temperature in nitrogen atmosphere, washed with deionized water followed by ethanol and dried at 60 °C for 3 h in a vacuum oven. The prepared catalysts were denoted as Ni–P–X–T, where X and T represented the molar ratio of $H_2PO_2^-/Ni^{2+}$ in the precursor and the thermal treatment temperature, respectively.

2.2. Catalyst characterization

X-ray diffraction (XRD) measurements were carried on a D/max2550 18KW rotating anode X-ray diffractometer with monochromatic Cu Kα radiation (λ = 1.5418 Å) at a voltage and a current of 40 kV and 300 mA, respectively. The crystallite size of the sample was quantified from the XRD pattern using the whole pattern fitting method. The specific surface area was measured by a Quantachrome's NOVA-2100e Surface Area instrument by physisorption of nitrogen at −196 °C. The elemental content of the sample was identified by inductively coupled plasma analysts (ICP) on a Varian VISTAMPX. The morphologies of catalysts were determined by transmission electron microscopy (TEM) on a JEOL JEM-2100 transmission electron microscope with a lattice resolution of 0.19 nm and an accelerating voltage of 200 kV.

2.3. Catalyst activity measurement

The HDO activity tests were carried out in a 300-mL sealed autoclave. The prepared catalyst (0.15 g) without any further treatment, p-cresol (13.5 g) and dodecane (86.5 g) were placed into the autoclave. Air in the autoclave was evacuated by pressurization–depressurization cycles with nitrogen and subsequently with hydrogen. The system was heated to desired temperature then pressurized with hydrogen to 4.0 MPa and adjusted the stirring speed to 900 rpm. During the reaction, liquid samples were withdrawn from the reactor and analyzed by Agilent 6890/5973 N GC-MS and 7890 gas chromatography using a flame ionization detector (FID) with a 30-m AT-5 capillary column. For the HDO of phenols, there exist two main pathways involving direct C–O bond rupture (DDO route), yielding aromatic products, and the other via the pre-hydrogenation of the aromatic ring producing cycloalkenes and cycloalkanes (HYD route). The DDO/HYD ratio and deoxygenation rate for each experiment were calculated as follows:

$$\mathrm{DDO/HYD} = \frac{\text{moles of methylbenzene}}{\text{moles of methylcyclohexane and 3-methylcyclohexene}}$$

$$\text{Deoxygenation rate (wt\%)} = \left(1 - \frac{\text{oxygen content in the final organic compounds}}{\text{total oxygen content in the initial material}}\right) \times 100\,\%$$

3. Results and discussion

3.1. Characterization of the Ni–P catalysts

Fig. 1(a) shows the powder XRD patterns of Ni–P catalysts prepared with different ratio of $H_2PO_2^-/Ni^{2+}$. The thermal decomposition of $H_2PO_2^-$ usually undergoes disproportionation reactions to produce PH_3, P, PO_3^{2-} and PO_4^{3-}, in which the low valent products such as PH_3 and P can reduce Ni^{2+} to form Ni_2P [23]. Ni-P-1-300 presented several sharp diffraction peaks at 2θ = 40.6°, 44.5°, 47.3°, 54.0°, 54.9° and 74.6°, attributing to the 111, 201, 210, 002, 211 and 400 reflections of the crystalline Ni_2P (JCPDS No. 74-1385) [27]. It indicated that Ni-P-1-300 had a good crystallinity. When the ratio of $H_2PO_2^-/Ni^{2+}$ was increased to 3 or 5, some slight peaks corresponding to Ni_5P_4 was observed, besides the main phase of Ni_2P, but the peak intensity of Ni_2P was increased, which indicated that the crystallite size of Ni–P catalysts calculated from the XRD pattern was increased by increasing the ratio of $H_2PO_2^-/Ni^{2+}$. However, when the ratio of $H_2PO_2^-/Ni^{2+}$ was increased to 10, the peak intensity of Ni_2P was decreased greatly, but the intensities of peaks of Ni_5P_4 was increased. These suggested that the main phase was transferred from Ni_2P to Ni_5P_4, which was resulted from that the high ratio of $H_2PO_2^-/Ni^{2+}$ provided excessive PH_3 for other reactions [25].

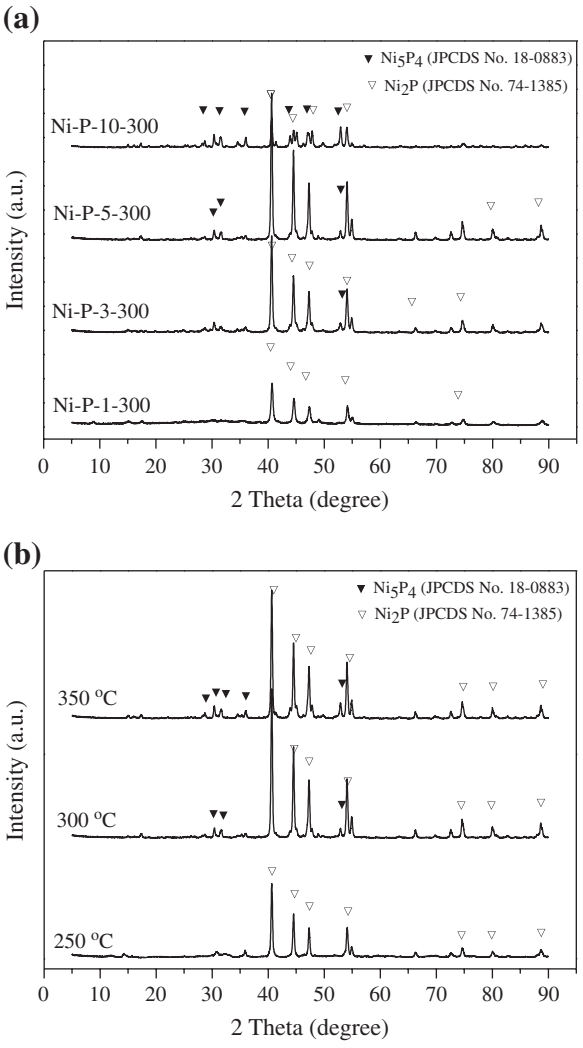

Fig. 1. XRD patterns of Ni–P catalysts prepared (a) with different ratio of $H_2PO_2^-/Ni^{2+}$ and (b) under different temperature.

The effects of thermal temperature on the sample phases are shown in Fig. 1(b). The peak intensity of Ni_2P was increased firstly and then decreased when the temperature rose from 250 °C to 350 °C. Heat treatments at high temperatures (300 °C and 350 °C) led to the formation of Ni_5P_4, besides the main phase of Ni_2P. This was mainly caused by the following reason. At the higher reaction temperature, the disproportionation of $H_2PO_2^-$ was very faster, leading to generate adequate PH_3 for the formation of Ni_5P_4, especially at 350 °C [23]. Therefore, there had optimum reaction temperature and $H_2PO_2^-/Ni^{2+}$ ratio for the maximum pure Ni_2P with big crystallite size.

The morphologies of Ni–P catalysts were observed by TEM and showed in Fig. 2. These TEM images showed that some particles aggregated each other in a certain extent, which might cause by a big surface energy of nano-particles. Many particles with the size of about 30–40 nm could be clearly seen in the TEM images of Ni-P-3-300 and Ni-P-5-300, but Ni-P-10-300 image displayed some blurry and irregular particles. The HRTEM image of Ni-P-5-300 showed many clear stripes. The distance of neighboring stripes was measured to be 0.51 nm. This was very close to 0.507 nm of (111) plane of Ni_2P form [25].

Specific surface areas and Ni/P atomic ratios of Ni–P catalysts prepared under different conditions are listed in Table 1. The temperature and the molar ratio of $H_2PO_3^-/Ni^{2+}$ did not affect the specific surface area significantly but obviously affect the Ni/P atomic ratio of Ni–P catalysts. The surface area of each as-prepared Ni–P catalyst was close to 6.0 m^2/g. All of Ni/P atomic ratios were lower than 2. It was also found that the Ni/P atomic ratio of Ni–P catalyst was decreased with the increases of the temperature and the $H_2PO_3^-/Ni^{2+}$ molar ratio. These suggested that other Ni–P species (e.g. Ni_5P_4) with lower Ni/P atomic ratio were generated. Hence, heating the precursor with low $H_2PO_3^-/Ni^{2+}$ molar ratio (1–3) at low temperature (250 °C) could obtain purer phase of Ni_2P.

Table 1
Surface area and composition of Ni–P catalysts.

Catalyst	Surface area (m^2/g)	Ni/P atomic ratio	Crystallite size (nm)
Ni-P-1-300	6.2	1.94	22.1
Ni-P-3-300	6.5	1.90	29.8
Ni-P-5-250	6.8	1.96	35.1
Ni-P-5-300	5.2	1.84	36.8
Ni-P-5-350	5.3	1.75	37.2
Ni-P-10-300	6.7	1.52	33.2

To investigate the valence state of Ni and P, Ni-P-5-300 catalyst was characterized the by XPS, as show in Fig. 3. Some oxides were unavoidably produced on the catalyst surface during the preparation and characterization. In the level of Ni 2p, the peak centered at 853.0 eV was attributed to $Ni^{\delta+}$ in the Ni_2P phase, and the peak at 856.4 eV corresponded to Ni^{2+} in surface NiO [28,29]. In the level of P 2p, two peaks around 129.6 and 133.7 eV were exhibited, corresponding to $P^{\delta-}$ in Ni_2P and P^{5+} in some surface phosphorus oxides [28,29]. These XPS results were well consistent with previous investigations [25,28,29].

3.2. Hydrodeoxygenation of p-cresol on Ni–P catalysts

The changes of p-cresol and product concentrations in the HDO of p-cresol on Ni-P-1-300, Ni-P-3-300, Ni-P-5-300 and Ni-P-10-300

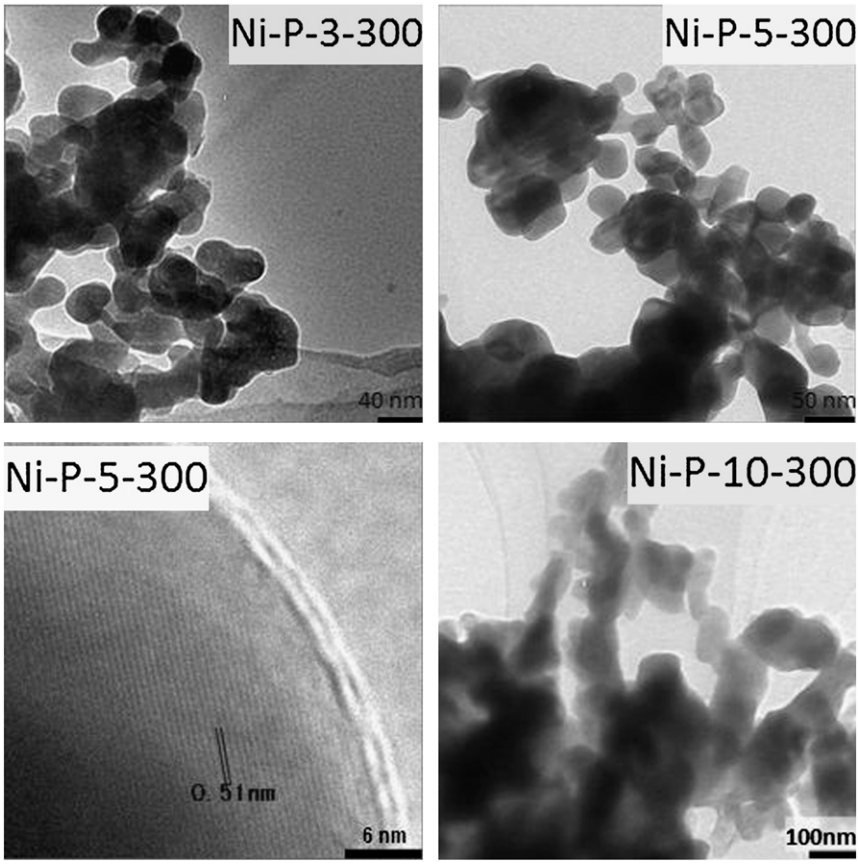

Fig. 2. TEM images of Ni–P catalysts.

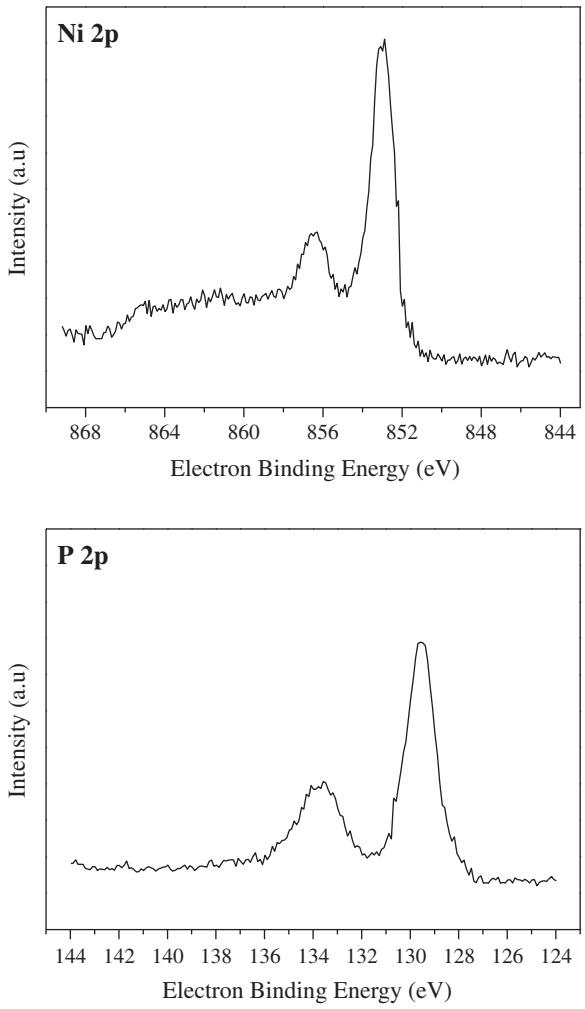

Fig. 3. XP spectra of Ni 2p and P 2p levels of Ni-P-5-300.

catalysts at 325 °C versus reaction time are displayed in Fig. 4. The HDO products were methylbenzene, methylcyclohexane and 3-methylcyclohexene without any oxygen-containing compounds. This indicated that Ni–P catalysts prepared by thermal decomposition method possessed high deoxygenation activity. According to the concentration of p-cresol, it was obvious to see that the activity of Ni–P catalyst was increased in the order of Ni-P-10-300 < Ni-P-1-300 < Ni-P-3-300 < Ni-P-5-300, indicating that the catalyst prepared with a suitable $H_2PO_3^-/Ni^{2+}$ molar ratio had the maximal HDO activity. Both the concentrations of methylbenzene and methylcyclohexane were increased with p-cresol conversion, and 3-methylcyclohexene in trace amounts was detected during reaction, which suggested that the reaction network for p-cresol HDO included two parallel pathways. One was proceeded by the pre-hydrogenation of the aromatic ring, the rapid elimination of water and the subsequent hydrogenation to aliphatic hydrocarbons (HYD route), and the other was the direct C–O bond scission yielding aromatic products (DDO route). To determinate whether methylcyclohexane and 3-methylcyclohexene were (all or partly) produced from the further hydrogenation of methylbenzene in H_2 atmosphere, the activity of Ni-P-5-300 in the hydrogenation of methylbenzene was tested under the same conditions as the HDO of p-cresol. The results showed that the conversion of methylbenzene to methylcyclohexane or 3-methylcyclohexene at the end of a 10-h run was only 5.0%. In addition, the previous study has found that the hydrogenation of p-cresol was easier than the hydrogenation of methylbenzene [30]. Under the presence of p-cresol, the hydrogenation of methylbenzene would be much slower due to the competitive adsorption of p-cresol on the catalyst surface. Therefore, the hydrogenation of methylbenzene was concluded to be negligible under the studied conditions. Şenol et al. [19] had also reported this similar result. Compared with the DDO/HYD ratio, it showed that the p-cresol HDO proceeded with the DDO pathway being the primary route for Ni-P-10-300 while Ni-P-5-300 favored the HYD pathway.

The effects of reaction temperature on the HDO of p-cresol over Ni-P-5-300 were summarized in Table 2. Both the conversion and the deoxygenation rate were increased with temperature, indicating that high temperature was beneficial to deoxygenation in the measured range. However, it does not completely true that the higher temperature corresponded to the higher conversion. Our previous study had revealed that there exists an exothermic reversible reaction equilibrium effect in the reaction networks for the HDO of p-cresol based on a thermodynamic calculation [31]. Compared with Ni-P-5-300 catalyst, when the thermal decomposition temperature was decreased to 250 °C or increased to 350 °C, the prepared catalyst showed lower conversion but higher HYD selectivity. The deoxygenation rate on Ni-P-5-250 and Ni-P-5-350 was 66.1% and 72.1%, respectively, being lower than that on Ni-P-5-300. Therefore, it could conclude that there existed an optimal thermal decomposition temperature to make the Ni–P catalyst to be the maximum activity.

As shown in Table 1, for the different thermal decomposition temperature, the crystallite size of these catalyst decreases with the order of Ni-P-5-350 (37.2 nm) > Ni-P-5-300 (36.8 nm) > Ni-P-5-250 (35.1 nm) while the Ni/P atomic ratio decreases in the order of Ni-P-5-250 (1.96) > Ni-P-5-300 (1.84) > Ni-P-5-350 (1.75). From Table 2, Ni-P-5-300 exhibited the highest activity and Ni-P-5-250 showed the lowest activity in the HDO of p-cresol. It seems that the big crystallite size of the Ni–P catalyst corresponds to the high HDO activity, which might be explained by the following reason. The relatively larger particle size facilitates the adsorption of p-cresol and thus was favorable for the conversion of p-cresol [32]. However, the Ni/P atomic ratio of the catalyst also had a great effect on its HDO activity. Compared with Ni-P-5-300, Ni-P-5-350 exhibited lower HDO activity, which was resulted from the lower Ni/P atomic ratio causing by the more Ni_5P_4. Form the crystallite size, Ni/P atomic ratio and HDO activity of Ni–P catalysts prepared with different of $H_2PO_2^-/Ni^{2+}$ molar ratio, it could also be concluded that the HDO activity depended on the crystallite size and Ni/P atomic ratio. For example, Ni-P-1-300 had smaller crystallite size but displayed higher HDO activity than Ni-P-10-300. Therefore, the bigger crystallite size and the purer phase of Ni_2P contributed to its higher HDO activity.

4. Conclusion

Unsupported Ni–P catalysts were directly synthesized by thermal decomposition method. The prepared conditions had little effect on the surface area of the catalyst but great effect on its purity and crystallite size. Heating the precursor with a suitable $H_2PO_3^-/Ni^{2+}$ molar ratio at low temperature (250 °C) could obtain pure phase of Ni_2P with a small crystallite size. The HDO of p-cresol on these Ni–P catalysts reacted though two parallel pathways: hydrogenation and dehydration route (HYD) and direct deoxygenation route (DDO), and the ratio of DDO/HYD was changed with the $H_2PO_3^-/Ni^{2+}$ molar ratio in the precursor and the thermal decomposition temperature. The conversion and the deoxygenation rates were reached to 85.0% and 83.4%, respectively. Ni-P-5-300 exhibited higher HDO catalytic

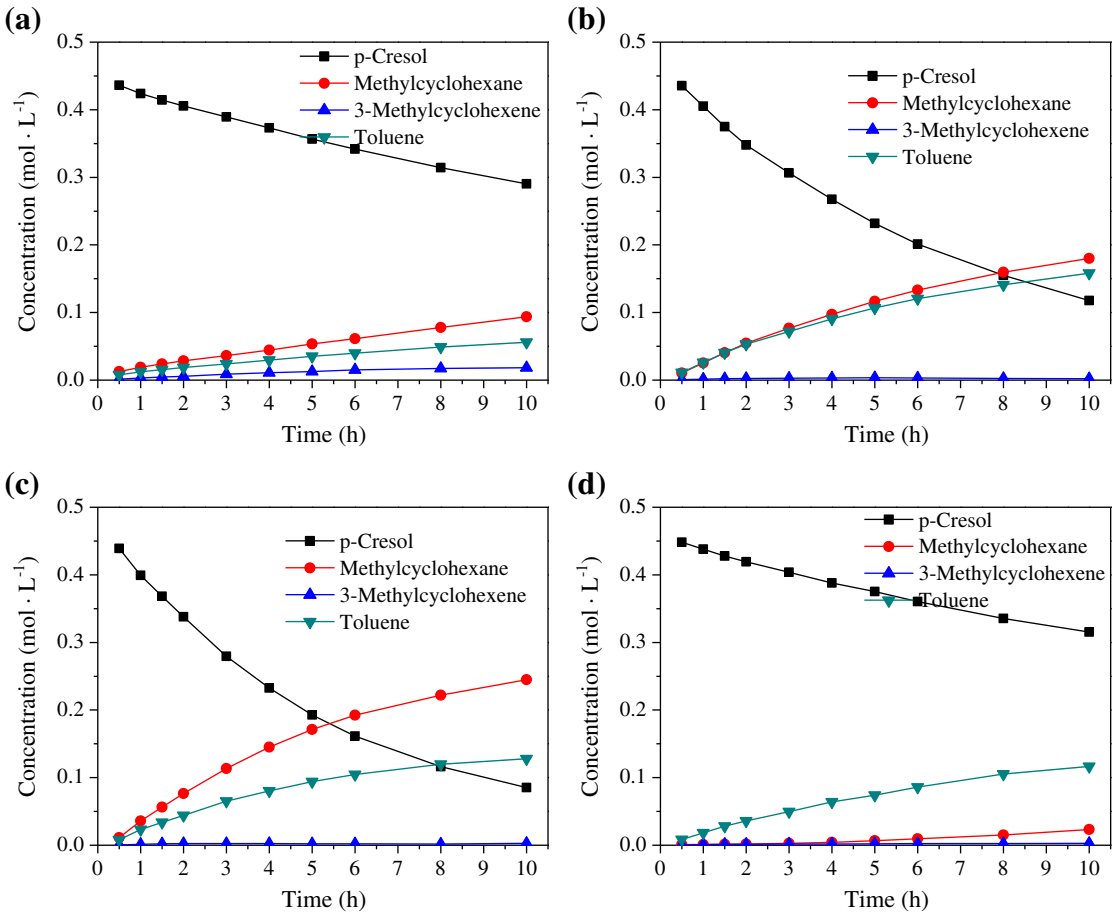

Fig. 4. The HDO of p-cresol on (a) Ni-P-1-300, (b) Ni-P-3-300, (c) Ni-P-5-300 and (d) Ni-P-10-300 catalysts. Reaction conditions: initial concentration of p-cresol 0.46 mol/L, 0.20 g catalyst, temperature 325 °C.

Table 2
The HDO of p-cresol on Ni–P catalysts at different temperature.[a]

Catalyst	Ni-P-5-300			Ni-P-5-250	Ni-P-5-350
	300 °C	325 °C	350 °C	325 °C	325 °C
Conversion (mol%)	73.2	81.4	85.0	68.5	74.3
HDO product distribution (mol%)					
Methylbenzene	35.2	34.3	34.0	17.4	26.0
3-Methylcyclohexene	1.3	0.8	0.2	1.1	2.5
Methylcyclohexane	63.5	64.9	65.8	81.5	71.5
DDO/HYD	0.54	0.53	0.52	0.21	0.35
Deoxygenation rate (wt%)	70.8	79.6	83.4	66.1	72.1

[a] Reaction conditions: p-cresol 13.5 g, dodecane 86.5 g, 0.20 g catalyst, $P(H_2) = 4.0 \times 10^6$ Pa, stirring speed 900 r/min, time 10 h.

activity than other Ni–P catalysts, which was attributed to its bigger crystallite size and purer phase of Ni_2P.

Acknowledgements

This research was supported by a specialized research fund for the Doctoral Program of Higher Education (20124301120009), the Natural Science Foundation of Hunan Province (13JJ4048), the National Students' Innovation and Entrepreneurship Training Program (201210530011) and the Scientific Research Fund of Hunan Provincial Education Department (12C0392).

References

[1] J.C. Serrano-Ruiz, J.A. Dumesic, Energy and the Environmental Science 4 (2011) 83–99.
[2] T.P. Vispute, H. Zhang, A. Sanna, R. Xiao, G.W. Huber, Science 330 (2010) 1222–1227.
[3] J. Zakzeski, P.C.A. Bruijnincx, A.L. Jongerius, B.M. Weckhuysen, Chemistry Review 110 (2010) 3552–3599.
[4] G.W. Huber, S. Iborra, A. Corma, Chemistry Review 106 (2006) 4044–4098.
[5] Q. Bu, H. Lei, A.H. Zacher, L. Wang, S. Ren, J. Liang, Y. Wei, Y. Liu, J. Tang, Q. Zhang, R. Ruan, Bioresource Technology 124 (2012) 470–477.
[6] C.R. Lee, J.S. Yoon, Y.-W. Suh, J.-W. Choi, J.-M. Ha, D.J. Suh, Y.-K. Park, Catalysis Communications 17 (2012) 54–58.
[7] P.T.M. Do, A.J. Foster, J. Chen, R.F. Lobo, Green Chemistry 14 (2012) 1388–1397.
[8] C. Wang, Z. Wu, C. Tang, L. Li, D. Wang, Catalysis Communications 32 (2013) 76–80.
[9] V.N. Bui, D. Laurenti, P. Delichère, C. Geantet, Applied Catalysis B: Environmental 101 (2011) 246–255.
[10] K. Li, R. Wang, J. Chen, Energy & Fuels 25 (2011) 854–863.
[11] H.Y. Zhao, D. Li, P. Bui, S.T. Oyama, Applied Catalysis A: General 391 (2011) 305–310.
[12] X. Zhang, T. Wang, L. Ma, Q. Zhang, Y. Yu, Q. Liu, Catalysis Communications 33 (2013) 15–19.
[13] C. Zhao, J.A. Lercher, 51 (2012) 5935–5940.
[14] W. Lai, L. Pang, J. Zheng, J. Li, Z. Wu, X. Yi, W. Fang, L. Jia, Fuel Processing Technology 110 (2013) 8–16.
[15] Z. Contreras-Valdez, J.C. Mogica-Betancourt, A. Alvarez-Hernández, A. Guevara-Lara, Fuel 106 (2013) 519–527.
[16] E.W. Qian, S. Abe, Y. Kagawa, H. Ikeda, Chinese Journal of Catalysis 34 (2013) 152–158.
[17] G. Yu, Y. Zhou, Q. Wei, X. Tao, Q. Cui, Catalysis Communications 23 (2012) 48–53.
[18] P.E. Ruiz, B.G. Frederick, W.J. De Sisto, R.N. Austin, L.R. Radovic, K. Leiva, R. García, N. Escalona, M.C. Wheeler, Catalysis Communications 27 (2012) 44–48.
[19] O.I. Şenol, E.M. Ryymin, T.R. Viljava, A.O.I. Krause, Journal of Molecular Catalysis A: Chemical 277 (2007) 107–112.

[20] F. Sun, W. Wu, Z. Wu, J. Guo, Z. Wei, Y. Yang, Z. Jiang, F. Tian, C. Li, Journal of Catalysis 228 (2004) 298–310.
[21] Y. Yang, A. Gilbert, C. Xu, Applied Catalysis A: General 360 (2009) 242–249.
[22] P. Bui, J.A. Cecilia, S.T. Oyama, A. Takagaki, A. Infantes-Molina, H. Zhao, D. Li, E. Rodríguez-Castellón, A. Jiménez López, Journal of Catalysis 294 (2012) 184–198.
[23] G. Shi, J. Shen, Journal of Materials Chemistry 19 (2009) 2295–2297.
[24] Q. Guan, W. Li, M. Zhang, K. Tao, Journal of Catalysis 263 (2009) 1–3.
[25] L. Song, S. Zhang, Q. Wei, Catalysis Communications 12 (2011) 1157–1160.
[26] Q. Guan, W. Li, Catalysis Science & Technology 2 (2012) 2356–2360.
[27] Y. Chen, H. She, X. Luo, G.-H. Yue, D.-L. Peng, Journal of Crystal Growth 311 (2009) 1229–1233.
[28] Y. Zhao, Y. Zhao, H. Feng, J. Shen, Journal of Materials Chemistry 21 (2011) 8137–8145.
[29] L. Song, S. Zhang, Q. Wei, Powder Technology 212 (2011) 367–371.
[30] W. Wang, Y. Yang, H. Luo, T. Hu, W. Liu, Catalysis Communications 12 (2011) 436–440.
[31] Y. Yang, H.a. Luo, G. Tong, K.J. Smith, C.T. Tye, Chinese Journal of Chemical Engineering 16 (2008) 733–739.
[32] B. Coq, F. Figueras, Coordination Chemistry Reviews 178–180 (1998) 1753–1783.